The Astrophysical Journal, 775:66 (10pp), 2013 September 20 doi:10.1088/0004-637X/775/1/66

HUBBLE SPACE TELESCOPE AND GROUND-BASED OBSERVATIONS OF V455 ANDROMEDAE POST-OUTBURST*

Paula Szkody[1], Anjum S. Mukadam[1], Boris T. Gänsicke[2], Arne Henden[3], Edward M. Sion[4], Dean M. Townsley[5], Damian Christian[6], Ross E. Falcon[7], Stylianos Pyrzas[8], Justin Brown[1], and Kelsey Funkhouser[1]
[1] Department of Astronomy, University of Washington, Box 351580, Seattle, WA 98195; szkody@astro.washington.edu, anjum@astro.washington.edu
[2] Department of Physics, University of Warwick, Coventry CV4 7AL, UK; boris.gaensicke@warwick.ac.uk
[3] AAVSO, 49 Bay State Road, Cambridge, MA 02138, USA; arne@aavso.org
[4] Department of Astronomy & Astrophysics, Villanova University, Villanova, PA 19085, USA; edward.sion@villanova.edu
[5] Department of Physics & Astronomy, University of Alabama, Tuscaloosa, AL 35487, USA; Dean.M.Townsley@ua.edu
[6] Department of Physics & Astronomy, California State University, Northridge, CA 91330, USA; damian.christian@csun.edu
[7] Department of Astronomy, University of Texas, Austin, TX 78712, USA; cylver@astro.as.utexas.edu
[8] Instituto de Astronomia, Universidad Catolica del Norte, Avenida Angamos 0619, Antofagasta, Chile; stylianos.pyrzas@gmail.com
Received 2013 June 27; accepted 2013 July 31; published 2013 September 5

ABSTRACT

Hubble Space Telescope spectra obtained in 2010 and 2011, 3 and 4 yr after the large amplitude dwarf nova outburst of V455 And, were combined with optical photometry and spectra to study the cooling of the white dwarf, its spin, and possible pulsation periods after the outburst. The modeling of the ultraviolet (UV) spectra shows that the white dwarf temperature remains ~600 K hotter than its quiescent value at 3 yr post-outburst, and still a few hundred degrees hotter at 4 yr post-outburst. The white dwarf spin at 67.6 s and its second harmonic at 33.8 s are visible in the optical within a month of outburst and are obvious in the later UV observations in the shortest wavelength continuum and the UV emission lines, indicating an origin in high-temperature regions near the accretion curtains. The UV light curves folded on the spin period show a double-humped modulation consistent with two-pole accretion. The optical photometry 2 yr after outburst shows a group of frequencies present at shorter periods (250–263 s) than the periods ascribed to pulsation at quiescence, and these gradually shift toward the quiescent frequencies (300–360 s) as time progresses past outburst. The most surprising result is that the frequencies near this period in the UV data are only prominent in the emission lines, not the UV continuum, implying an origin away from the white dwarf photosphere. Thus, the connection of this group of periods with non-radial pulsations of the white dwarf remains elusive.

Key words: binaries: close – novae, cataclysmic variables – stars: individual (V455 And, HS 2331+3905) – stars: oscillations

Online-only material: color figures

1. INTRODUCTION

V455 And is a unique cataclysmic variable that was first discovered in the Hamburg Quasar Survey (HS 2331+3905; Hagen et al. 1995). During follow-up observations since that time, it was discovered that V455 And contains one of the coolest white dwarfs among all cataclysmic variables, implying a very low secular mean accretion rate (Townsley & Gänsicke 2009). The data also identified six different periodicities (Araujo-Betancor et al. 2005, hereafter AB05; Gänsicke 2007; Bloemen et al. 2013). Partial eclipses in the optical light curve revealed an inclination near ~75° and an orbital period of 81.08 minutes, near the period minimum (Gänsicke et al. 2009), while a photometric period at 83.38 minutes was also evident, ascribed to superhumps in a precessing disk. A longer spectroscopic period of 3.5 hr that drifts on timescales of days was observed. A stable short period at 67.62 s and its second harmonic ($2f$) were found from Discrete Fourier Transforms (DFTs) of long data sets, and attributed to the rotation of the white dwarf, thus identifying this system as an Intermediate Polar (IP).[9] In addition, a beat period from the spin and the spectroscopic period (at 67.25 s) and its harmonic were visible. Lastly, a broad range of periods between 300–360 s was apparent during quiescence and attributed to non-radial pulsations of the white dwarf. The width of this broad feature could be due to unresolved multiplets or a lack of coherence.

As a dwarf nova, V455 And was observed to have an outburst in 2007 September when it increased in brightness by 8 mag (Samus et al. 2007; Broens et al. 2007). Like all short orbital period dwarf novae, the outbursts are infrequent and of high amplitude (Howell et al. 1995). The short period is likely the reason why this system is unique among IPs in having such a high-amplitude outburst and a visible white dwarf. This sole outburst provides an opportunity to study the heating of a white dwarf from the outburst (Godon et al. 2006; Piro et al. 2005) and its subsequent cooling, as well as the effect of the outburst on the possible non-radial pulsation. Single, non-accreting white dwarfs take evolutionary timescales (millions of years) to cool across the instability strip (Kepler et al. 2005; Mukadam et al. 2013), whereas dwarf novae outbursts allow a study of cooling on timescales of a few years (Mukadam et al. 2011b; Szkody et al. 2012).

Since the accretion disk contaminates the optical light of dwarf novae at quiescence, the UV is the best wavelength regime to determine the parameters of the white dwarf. An UV spectrum of V455 And obtained during a snapshot program with the Space Telescope Imaging Spectrograph (STIS) during

* Based on observations made with the NASA/ESA *Hubble Space Telescope*, obtained at the Space Telescope Science Institute, which is operated by the Association of Universities for Research in Astronomy, Inc., (AURA) under NASA contract NAS 5-26555, with the Apache Point Observatory (APO) 3.5 m telescope, which is owned and operated by the Astrophysical Research Consortium (ARC), and the McDonald Observatory 2.1 m telescope which is owned and operated by the University of Texas at Austin.

[9] asd.gsfc.nasa.gov/Koji.Mukai/iphome/catalog/alpha.html

Table 1
Summary of *HST* and Related Optical Observations

Date	Obs	Filter	Exp (s)	UT Time
2010 Oct 2	APO	DIS	600	04:48–04:58
2010 Oct 12	FTN	*g*	10	08:02:02–12:54:40
2010 Oct 14	McD	BG40	5	02:56:59–09:23:39
2010 Oct 14	FTN	*g*	10	08:02:48–12:34:47
2010 Oct 14	*HST*	G160M	···	13:03:22–13:43:22
2010 Oct 14	*HST*	G140L	···	19:27:22–20:15:22
2010 Oct 15	McD	BG40	10	06:47:09–07:50:59
2010 Oct 15	McD	BG40	5	07:53:38–09:00:48
2010 Oct 16	FTN	*g*	10	06:22:36–07:21:50
2010 Oct 18	McD	BG40	5	05:09:16–05:54:36
2011 Sep 25	APO	BG40	5	01:48:31–12:17:56
2011 Sep 25	*HST*	G140L	···	12:33:48–13:05:48
2011 Sep 25	*HST*	G140L	···	14:09:48–14:57:58
2011 Sep 26	APO	BG40	5	01:50:48–07:04:48

quiescence in 2002 (AB05) was modeled with a white dwarf at a temperature of $10{,}500 \pm 250$ K along with broad emission lines from an accretion disk viewed at high inclination. A distance of 90 ± 15 pc was provided by the model fit. Unfortunately, this spectrum was too short (700 s) to do any analysis for pulsations.

Our *Hubble Space Telescope* (*HST*) and optical monitoring program was designed to determine the post-outburst cooling of the white dwarf as well as to study the effects of heating during outburst and subsequent cooling on the observed periods.

2. OBSERVATIONS AND DATA REDUCTION

Two sets of *HST* observations (2010 October 14 and 2011 September 25) with coordinated ground optical observations were obtained 3 and 4 yr after outburst. The details are provided below, and a summary of the observations is presented in Table 1. Photometric data have also been collected since 2007 that allow for a comparison of the data acquired in coordination with the *HST* observations to that at quiescence (2003) and further from outburst. These data are summarized in Table 2.

2.1. HST Observations

The 2010 observation was scheduled for five orbits using the Cosmic Origins Spectrograph (COS), with the first four using the G160M grating and the last one with the G140L grating. Unfortunately, the pointing was lost on the middle three orbits, so only the first and last data sets could be used. The G160M spectra cover 1388–1559 Å and 1577–1748 Å with a resolution of about 0.07 Å, and the G140L spectra cover 1130–2000 Å with a resolution of about 0.75 Å. The time span of the good data resulted in orbital phase coverage of 0.18–0.68 for G160M and 0.92–0.51 for G140L, using the ephemeris provided in AB05. In 2011, there were two COS orbits with G140L, covering orbital phases of 0.46–0.86 and 0.65–0.25.

All data were obtained in time-tag mode and analyzed using PyRAF routines from the STSDAS package HSTCOS (version 3.14). From trials of various extraction widths to optimize the signal-to-noise ratio (S/N), the best values of 27 pixels for the G160M and 41 pixels for the G140L were used. Different light curves were created by binning over 1–5 s timescales and summing over different wavelength regions, i.e., with and without emission lines. To search for periodic variability via DFT analysis, these light curves were changed into fractional amplitude by dividing by the mean and then subtracting one.

Table 2
Summary of Long-term Optical Monitoring Observations

Date	Obs	Filter	Total Hours
2003 Aug 14–20	Kry	clear, *V*	24.8
2007 Oct 17	APO	BG40	1.5
2008 Sep 6–8	APO, McD	BG40	8.3
2009 Oct 7–9	Kry	clear	13.0
2010 Sep 7–12	APO, McD	BG40	17.5
2010 Oct 11–18	FTN, McD	*g*, BG40	17.7
2011 Sep 25–26	APO	BG40	15.7
2012 Jul 21	APO	BG40	3.8
2012 Aug 5	MRO	BG40	4.9
2012 Oct 13	APO	BG40	10.6

The best-fit periods were determined by subjecting the fractional intensity light curve to least-squares fitting. An empirical method used in past data analysis (Kepler 1993) was employed to find the 3σ limit of the noise. This involved subtracting the best-fit periods, shuffling the residual intensities to obtain a pure white-noise light curve, using the DFT of this light curve to obtain an average (1σ) amplitude, and then repeating this 10 times to derive the 3σ value. Computing the 3σ white-noise limit enables confidence that the signal was not randomly generated, and determines which peaks in the DFT can be safely ignored.

2.2. Optical Data

Ground-based optical telescope time was coordinated with the *HST* observations. The American Association of Variable Star Observers (AAVSO) monitored the brightness for weeks preceding both *HST* scheduled times (these data can be viewed from their archive site[10]). In 2010, three nights of observations with the Las Cumbres Observatory Global Telescope Network 2 m Faulkes Telescope North (FTN) were obtained on October 12, 14, and 16. The Merope CCD was used with a Sloan Digital Sky Survey *g* filter and 10 s integrations on October 12, while the Spectral CCD was used on October 14 and 16. The 2.1 m telescope at McDonald Observatory (McD) obtained data on October 14, 15, and 18 using the Argos CCD camera (Nather & Mukadam 2004) with a BG40 filter and 5–10 s integrations. The 3.5 m telescope at Apache Point Observatory (APO) obtained a 10 minute spectrum on October 2 using the Double Imaging Spectrograph (DIS) in low-resolution mode (coverage of 3800–9000 Å at a resolution of about 4.8 Å in the blue and about 9 Å in the red).

In 2011, the Agile CCD camera (Mukadam et al. 2011a) with a BG40 filter was used at the APO 3.5 m with 5 s integrations on September 25 and 26 to obtain light curves. These data were presented in Silvestri et al. (2012) but were inadvertently labeled with the year 2010 instead of 2011.

In addition to the ground observations coincident with the *HST* observations, long-term photometric monitoring was also accomplished with these facilities as well as the University of Washington Manastash Ridge Observatory (MRO) 0.76 m telescope using a 1024 × 1024 SITe CCD with a BG40 filter, and the 1.2 m Kryoneri telescope in Korinth, Greece, using a 516 × 516 Photometrics CCD with either a *V* filter or no filter (Table 2).

[10] http://www.aavso.org

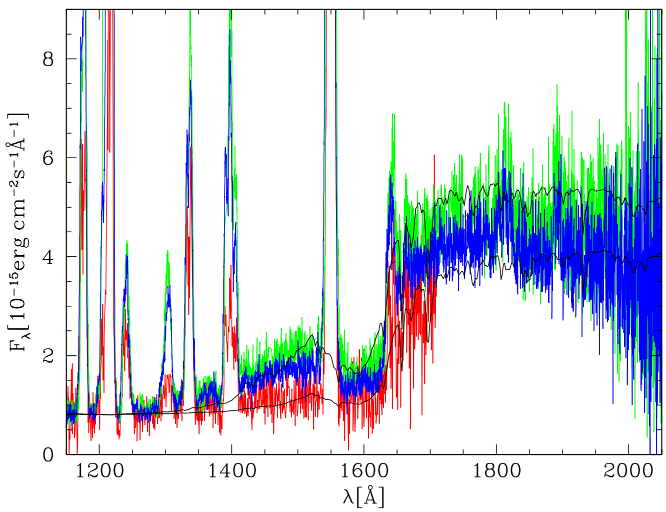

Figure 1. COS G140L data from 2010 October 14 (top, green), 2011 September 25 (middle, blue), and STIS data from 2002 (bottom, red). Black lines are models for 10,600 K (bottom) and 11,100 K (top).

(A color version of this figure is available in the online journal.)

The CCD data were analyzed using IRAF[11] routines to flat field and bias correct the images and obtain sky-subtracted count rates for V455 And and comparison stars on the same frames. The mid-integration times were extracted from the headers and converted to Barycentric Dynamic Time. The light curves that were then created were treated in the same manner as the *HST* light curves, with a conversion to fractional intensity for computing DFTs, and subsequent least-squares analysis to determine the best-fit periods and establish the 3σ noise limit.

3. RESULTS

The spectra were analyzed for temperature changes in the white dwarf as well as for system periodicities in comparison to the parameters of V455 And at quiescence.

3.1. White Dwarf Temperatures

The COS G140L spectra obtained at 3 and 4 yr after the dwarf nova outburst exhibit the sharp upturn in flux at long wavelengths and the quasi-molecular H_2 absorption at 1600 Å that are typical of a cool white dwarf. These spectra are plotted along with the STIS spectrum obtained at quiescence (AB05) in Figure 1. The increased continuum even at 4 yr after outburst is evident, along with strong emission lines of C IV, C III, C II (1550, 1175, 1335 Å), Si IV, Si III (1400, 1300 Å), N V (1240 Å), and He II (1640 Å). Using the same model spectra that were calculated from Hubeny (1988) and Hubeny & Lanz (1995) in AB05, and fixing the same gravity to $\log g = 8.0$ and photospheric abundances to 0.1 solar, a temperature of 11,100 K was determined for the 2010 data. Figure 1 shows the contributions of 11,100 and 10,600 K white dwarfs. The 2011 spectra fall in-between these values. The error bars on the fits are on the order of ±250 K due to the sensitivity of the temperature to the quasi-molecular H_2 absorption at 1600 Å. While the lack of knowledge of the source and contribution of the far-ultraviolet (FUV) emission impact all the fits, it is clear that the temperature and UV flux are elevated from the quiescent values. The low temperature of the white dwarf in V455 And is consistent with that expected for a 0.6 $M_\odot$ white dwarf at its orbital period, with a time-averaged accretion rate $\sim 3 \times 10^{-11}$ $M_\odot$ yr^{-1} as expected from angular momentum losses from gravitational radiation (Figure 3 in Townsley & Bildsten 2003).

[11] IRAF is distributed by the National Optical Astronomy Observatory, which is operated by the Association of Universities for Research in Astronomy, Inc., under cooperative agreement with the National Science Foundation.

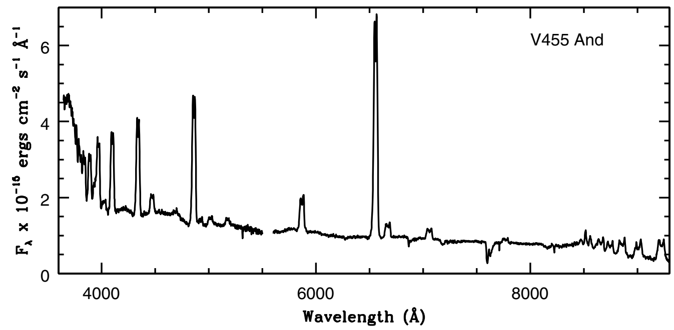

Figure 2. APO spectra obtained 2010 October 2. Short gap near 5500 Å marks where the dichroic separates the blue and red spectra.

Table 3
Emission Line Equivalent Widths (Å)

Line (Å)	2010 Oct	2011 Sep	2002 Oct[a]
C III (1175)	81–118	77–135	111
N V (1240)	30–39	27–47	42
Si III (1300)	23–63	16–69	...
C II (1335)	52–72	48–76	67
Si IV (1400)	63–89	60–86	52
C IV (1550)	159–183	150–367	234
Hβ	84	...	75
Hα	225	...	185

Note. [a] Values from AB05 at quiescence.

The optical magnitudes provided by the AAVSO near the time of the 2010 observations were $V \sim 16.0$, while the quiescent magnitude reported in AB05 is $V \sim 16.4$. The variability of V455 And is on the order of 0.2 mag so the optical brightness (due to the accretion disk and heated white dwarf) is consistent with the increased continuum brightness in the UV at 3 yr past outburst. The optical spectrum obtained on 2010 October 2 (Figure 2) shows a similar spectrum to the quiescent one shown in AB05, albeit with slightly increased continuum, line equivalent widths (EWs; Table 3), and FWHM values (1678 and 2037 km s^{-1} for Hα and Hβ compared to 1312 and 1475 km s^{-1} in AB05). The most notable differences are in the stronger blue continuum shortward of 3800 Å and increased Hα flux. However, the comparison is not perfect as the spectrum shown in AB05 is an average of many spectra over an orbit while Figure 2 is only one spectrum.

By 2011 September, the optical brightness ranged from 16.0 to 16.4, indicating values closer to pre-outburst. The two data sets indicate that the cooling time for the white dwarf in V455 And is greater than 4 yr.

Using the two temperatures from the COS *HST* spectra (11,100 ± 250 K and 10,850 ± 300 K), together with the corresponding days since outburst (1125 and 1471), and the quiescent temperature of $T_{\rm eff,0} = 10{,}500$ K, the formulation given in Piro et al. (2005) allows an estimate of the mass accreted in the outburst. Due to the power-law nature of the late-time cooling, as shown in Equation (20) of Piro et al. (2005), $\delta T/T_{\rm eff,0} = (t_{\rm late}/t)^{0.81}$, where $\delta T = T_{\rm eff}(t) - T_{\rm eff,0}$, the two temperature measurements during the cooling provide two

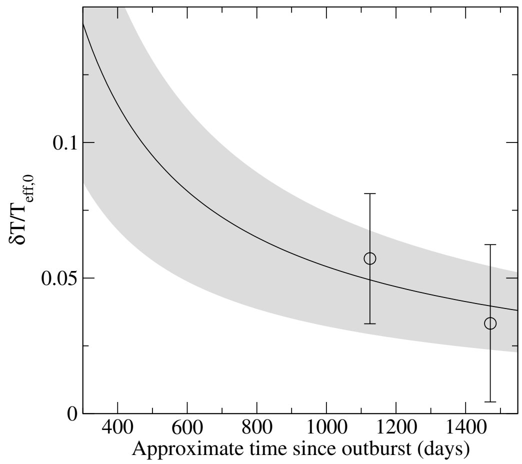

Figure 3. Cooling curve based on the two temperature measurements at 3 and 4 yr post-outburst and the quiescent temperature $T_{\mathrm{eff},0}$ from pre-outburst STIS data.

estimates of the late-time cooling timescale $t_{\mathrm{late}} = 33 \pm 14$ and 22 ± 19 days, for an average t_{late} of 27 ± 13 days. This estimated cooling curve and uncertainty band are shown in Figure 3. Using this average value along with $\log g = 8$ in Equation (22) of Piro et al. (2005) yields an accreted mass of $1.5 \pm 0.6 \times 10^{-9}\ M_{\odot}$. Due to the uncertainty of the white dwarf mass, this value likely has an additional uncertainty by a factor of two. This accreted mass is consistent with the upper limit obtained from EQ Lyn after its outburst (Mukadam et al. 2011b).

3.2. White Dwarf Velocity

While there are no metal absorption lines evident from the white dwarf in the UV spectrum (Figure 1), we attempted to obtain a velocity curve from the strong emission lines that are present. All the data from 2010 and 2011 were binned into 0.10 phase bins and the velocities of C III, N V, Si III, C II, Si IV, and C IV lines were measured using the centroid and Gaussian fitting routines under the *splot* routine in IRAF. The EWs of the lines are given in Table 3 along with the values at quiescence (from AB05). The quiescent values were obtained from a single 700 s STIS exposure, while our COS orbits cover 0.5 of the binary orbital period in 2010 and 0.7 in 2011. The phase coverage shows the large range in variation of the line strengths during the orbit. However, no consistent velocities could be determined at comparable phases between the two observation times, nor even at overlapping phases within the two *HST* orbits during each observation. This result is similar to that found from quiescent optical spectra that included orbital coverage, where AB05 found the dominant velocity variation in the lines to be near 3.5 hr. This long period was not coherent as it showed phase drifts of days. Our short data strings do not allow us to obtain adequate phase coverage of a 3.5 hr period, but it appears the UV lines do not originate in a region that is primarily involved in the orbital motion.

3.3. Periodicities in 2010 and 2011

The light curves and DFTs created from the COS and optical photometry obtained close in time to the UV data were searched for the spin and pulsation periods. Figure 4 shows the intensity light curve and DFT from the 2010 October 14 COS data (orbit 1 with G160M and orbit 5 with G140L) with time bins of 1 s and excluding the strong emission lines. Wavelength ranges of 1410–1535, 1579–1632, and 1648–1748 Å were used. The

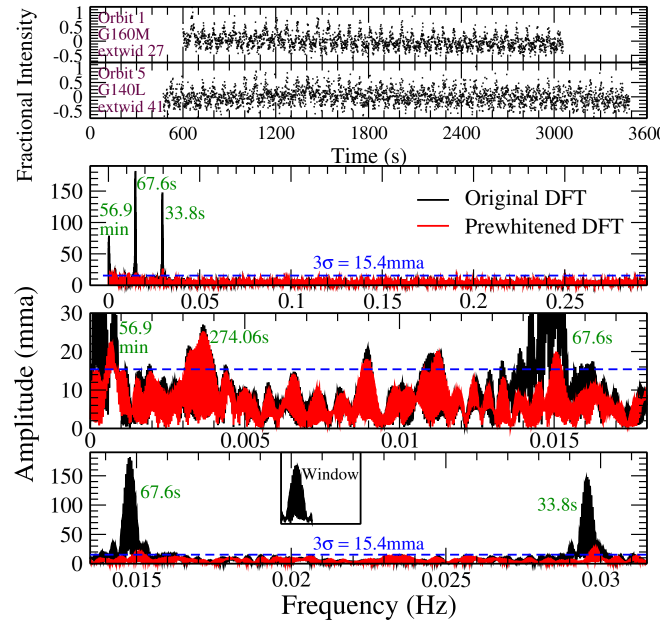

Figure 4. COS light curve from 2010 October 14 with 1 s exposures, using wavelength regions 1410–1535, 1579–1632, and 1648–1749 Å, excluding emission lines for orbit 1 (G160M) and orbit 5 (G140L). Fractional intensity (top), DFT (middle) with spin period (67.6 s), and second harmonic (33.8 s) labeled, and expanded high-frequency regions (bottom) with pulsation period (274 s) labeled.

(A color version of this figure is available in the online journal.)

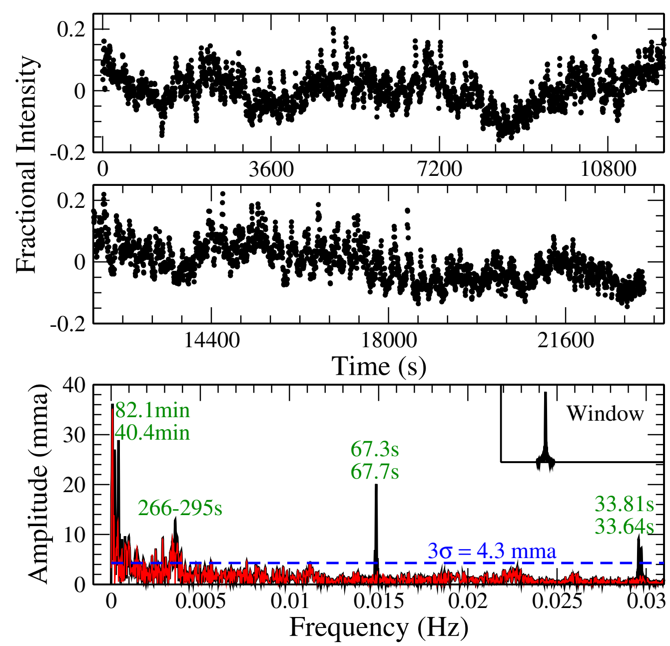

Figure 5. Light curve and DFT from McDonald 2010 October 14 with 5 s exposures and BG40 filter. Fractional intensity (top) and DFT (bottom).

(A color version of this figure is available in the online journal.)

prominent spin at 67.6 s and its second harmonic at 33.8 s are easily visible in the light curve and the DFT. A broad period around 274 s is visible in the expanded version of the DFT (middle panel) that is above the 3σ noise level of 15 mma. Figure 5 shows the optical data obtained the same night as the COS data. The 6 hr length of the optical data stream allows a good view of the superhump variability as well as the spin modulation. These periods show up easily in the DFT, as well

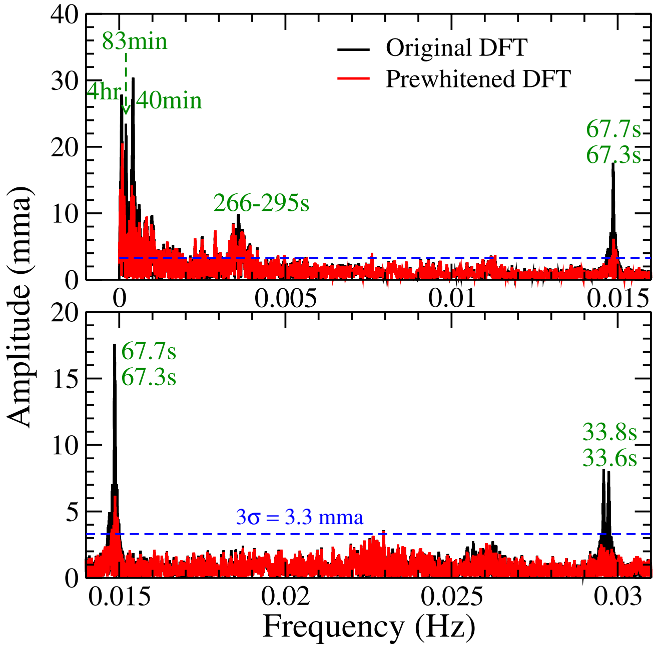

Figure 6. Combined DFT from 2010 October 12–18 showing the photometric period at 83 minutes, the pulse period at 276.5 s, and the spin and beat (67.7, 67.3 s) periods and their second harmonics.

(A color version of this figure is available in the online journal.)

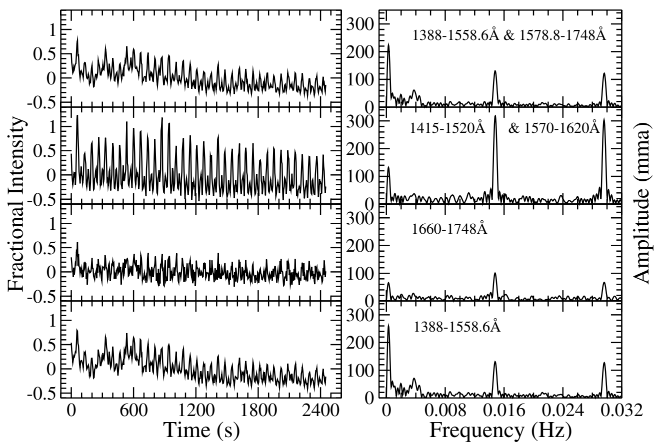

Figure 7. Light curves (left) and DFTs (right) of the first COS orbit with G160M on 2010 October 14 constructed with the different wavelength regions as labeled. The top and bottom panels include continuum and lines (the top is the entire range while the bottom is restricted to wavelengths where the white dwarf is negligible). The middle two panels are continuum only, with the third panel being wavelengths where the white dwarf dominates and the second where the other component of the FUV light dominates.

as a prominent broad period at about 280 s. Figure 6 shows the combined DFT of all the optical data (Table 1) obtained within a few days of the COS data. The broad pulsation period ranges from 266 to 295 s over the course of five days. Due to the similarity of this period to the 274 s one visible in the COS data, we made a first assumption that these periods originate from the same source. Further evidence for this assumption comes from the *Galaxy Evolution Explorer* (*GALEX*) near-UV (NUV; 1750–2800 Å) data obtained on 2010 August 26 and September 21 (Silvestri et al. 2012) where periods at 272 s (amplitude of 34 mma) on August 26 and 278 s (amplitude of 24 mma) on September 21 were evident.

In efforts to locate the source of the spin and pulsation periods, we created light curves at a variety of different wavelengths and

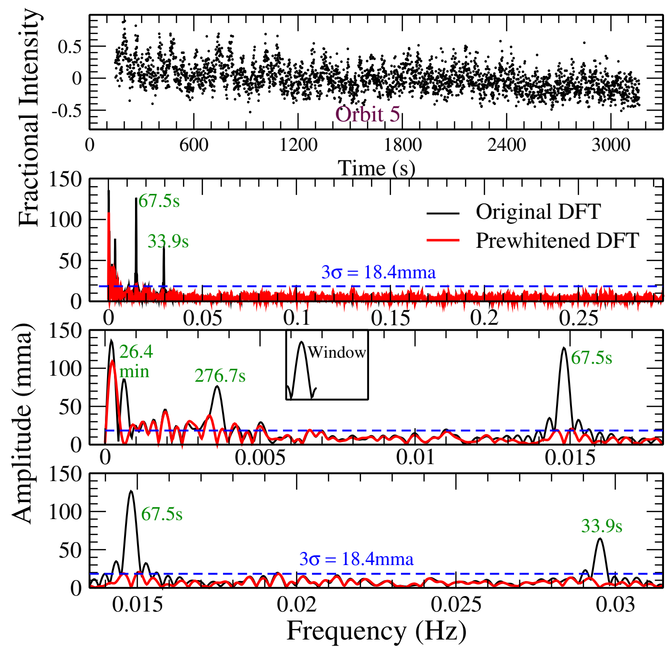

Figure 8. COS light curves from 2010 October 14 with 1 s exposures, using only wavelength regions containing emission lines (excluding Lyα). Fractional intensity (top), DFT (middle) with spin period (67.6 s) and second harmonic (33.8 s) labeled, and expanded high-frequency regions (bottom).

(A color version of this figure is available in the online journal.)

tried using pure continuum regions as well as pure emission line regions. Using the highest resolution G160M data, we sampled wavelengths shortward and longward of the upturn in the flux near 1650 Å (presumably due to the white dwarf flux distribution for its 11,000 K temperature; Figure 1). The resulting light curves and DFTs are shown in Figure 7. The top panels are for 340 Å that include lines and continuum regions over the entire available spectrum. The second panels cover 155 Å of the continuum blueward of the upturn excluding the emission lines. The third panels cover 90 Å of the longest wavelengths where the white dwarf contributes the most flux. The bottom panels cover 170 Å of the shortest wavelength regions including both continuum and lines. The FUV continuum below 1600 Å is precisely the region that AB05 could not explain with their model of a WD + 6500 K disk + L2 secondary star. This could be a hot disk, boundary layer, or magnetic interaction zone. The strongest amplitudes of the spin and its harmonic are evident in the wavelengths shorter than 1620 Å and have maximum amplitude in the continuum-only panels (second from top). Most surprisingly, the possible pulsation feature (near 0.0035 Hz) is evident only in the panels that contain emission lines as well as continua (top and bottom panels), and more importantly, it is absent from the continuum-only panels (second and third panels). These results imply that the origins of the spin as well as the pulse light are not directly from the photosphere of the white dwarf.

We also used the one orbit of G140L grating data to construct a light curve using only the emission lines (excluding Lyα which is primarily geocoronal), shown in Figure 8. This plot confirms the result from the G160M data by showing a much larger amplitude period at 276 s in the emission lines than in the continuum plot (Figure 4). We attempted to determine if the lines could result from the disk reprocessing of the pulsed light from the white dwarf by comparing the DFTs and phases of the blue versus the red wings of the combined emission lines. The results yielded

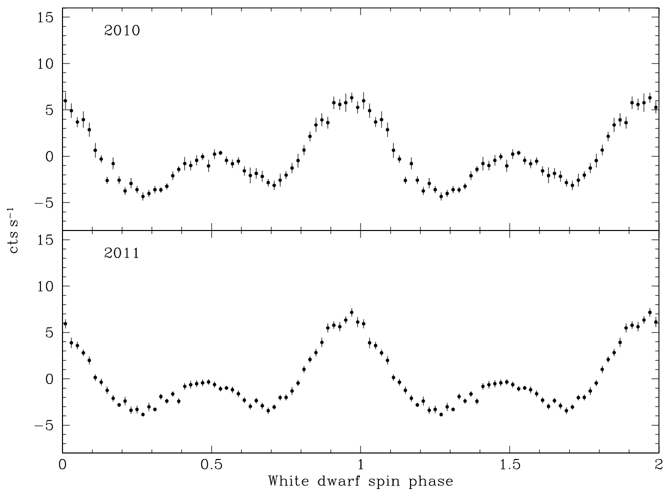

Figure 9. COS G140L light curves from UV continuum region 1420–1520 Å folded on the white dwarf spin period of 67.62 s and binned into 0.02 phase bins. The top panel is 2010 October 14 and bottom panel is 2011 September 25. Vertical scales are offset for plotting.

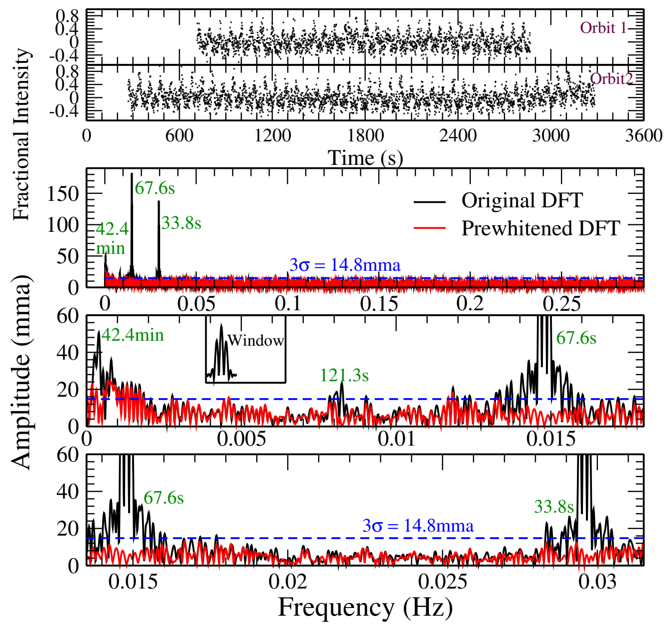

Figure 10. COS light curve from 2011 September 25 with 1 s exposures, using wavelength regions 1410–1535, 1579–1632, and 1648–1749 Å, excluding emission lines. Fractional intensity (top), DFT (middle) with spin period (67.6 s) and second harmonic (33.8 s) labeled, and expanded high-frequency regions (bottom).

(A color version of this figure is available in the online journal.)

a period difference of 20 s. When we force-fit with a single optimized period, then the phase difference obtained was 50 s. This implies much larger distances than the orbital separation and discounts reprocessing. However, we do not have sufficient photons in any one line nor sufficient orbital coverage to obtain a conclusive result. In the analysis of optical emission line data obtained only nine months after outburst, Bloemen et al. (2013) also reported excess power at 288 s in the periodogram created from the Hγ emission line. They observed this same period in the continuum between 4520 and 4670 Å, although at lower amplitude. However, they reported a different result for the spin amplitudes at that time, with a higher amplitude for the second harmonic of the spin in the lines than in the continuum.

Folding the white dwarf continuum data in the region of 1420–1520 Å on the spin period of 67.62 s and binning to 0.02 phase produce the light curve shown in the top panel of Figure 9. A clear double-hump modulation is apparent, consistent with two-pole accretion onto a magnetic white dwarf.

In the following year, on 2011 September 25, the two orbits of COS data with G140L excluding the emission lines (Figure 10) show only the prominent spin period and its second harmonic, with no obvious presence of the putative pulsation period in the UV continuum. The optical data obtained on the nights of September 25 and 26 (Figure 11) still show a broad range of periods between 273 and 349 s. The spin amplitudes show no change from the values in 2010. The stronger signal from the two orbits with the G140L grating and the closer timing of the two *HST* orbits in 2011 compared to the 2010 data (a combination of G160M and G140L separated by four *HST* orbits) should have allowed a better detection of the pulse period in the continuum. However, past UV data on several accreting pulsators at quiescence (Szkody et al. 2010) have shown that there can be no detection in the UV while variability attributed to pulsation is seen in the optical. While there is a small chance that these white dwarfs are exhibiting high-ℓ g-mode pulsations,[12]

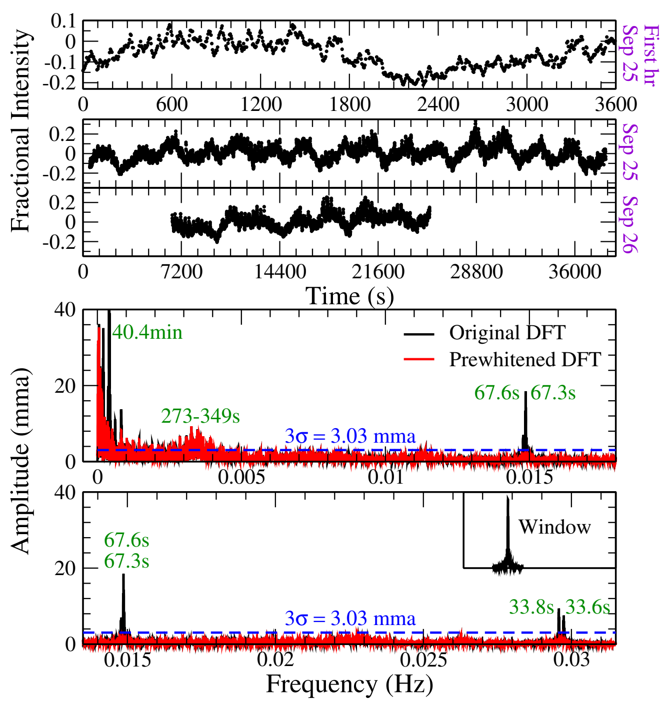

Figure 11. Light curves and DFTs from 2011 September 25 and 26 APO data. Top intensity curve is the expanded first hour of observations to show details of the light-curve variability.

(A color version of this figure is available in the online journal.)

the $\ell = 4$ modes do not show a significant change in amplitude as a function of wavelength and these modes have not been unambiguously identified in any of the known ZZ Ceti stars. It is also possible that the observed variability may be caused by a precessing disk which obscures the view of the white

[12] Non-radial g-mode pulsations observed in white dwarfs divide the stellar surface into zones of higher and lower effective temperature, depending on the degree of spherical harmonic ℓ, thus yielding lower optical amplitudes due to a geometric cancellation effect. Increased limb darkening at UV wavelengths ensures that modes with $\ell \leqslant 3$ are canceled less effectively, leading to higher amplitudes (Robinson et al. 1995).

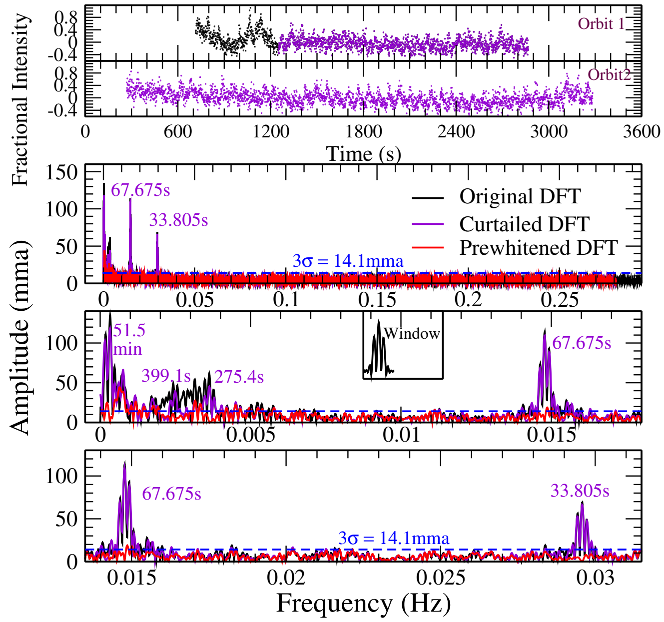

Figure 12. COS light curve from 2011 September 25 with 1 s exposures, using only wavelength regions containing emission lines (excluding Lyα). Fractional intensity (top), DFT (middle) with spin period (67.6 s) and second harmonic (33.8 s) labeled, and expanded high-frequency regions (bottom). Curtailed DFT is excluding the feature in the first 600 s of data in orbit 1.

(A color version of this figure is available in the online journal.)

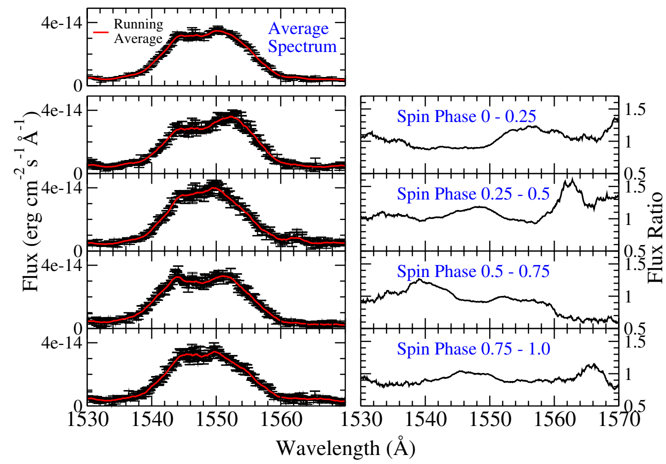

Figure 13. 2011 September 25 COS spectral profile of the C iv line phase-folded and binned at the spin period of 67.619 s (left panels), with the solid lines indicating a running average obtained over 2 Å (box length 25 points). Right-hand panels show these spin-phased spectra divided by the running average of the average line profile (solid line in top left panel). The lines change from red peaks (spin phase 0–0.25) to blue (spin phase 0.5–0.75) during the spin cycle.

(A color version of this figure is available in the online journal.)

dwarf. If the pulsation is somehow related to the interaction of a weak magnetic field with the inner disk, it is of note that the Intermediate Polar V842 Cen also shows an optical but not an UV period (Sion et al. 2013).

As with the 2010 data, a light curve was constructed using only the emission lines (except Lyα) from the two orbits of G140L in 2011 September. The result and the computed DFT are shown in Figure 12. Comparing this figure with Figure 10 (continuum only for the same data set) shows similar results as the previous year. The group of periods near 275 s that could be associated with a pulsation is apparent only in the DFT that isolated photons from the emission lines. This further reinforces the idea that the origin of this period is associated with material away from the white dwarf photosphere.

The spin and second harmonic are present in both the continuum and emission line DFTs but have reduced amplitudes in the emission line DFT versus the continuum DFT. The bottom panel of Figure 9 shows the 2011 continuum (1420–1520 Å) data folded on the spin period, revealing the same double-humped modulation as in the 2010 data. The topmost left panel of Figure 13 shows the average line profile of the C iv emission feature, while the lower left panels show the result of folding the data on the spin period and then binning into four bins based on spin phase. All the left panels show a running average (solid line) with reduced uncertainties computed over a box length of 25 points, corresponding to a wavelength bin of 2 Å. Following the analysis of Bloemen et al. (2013), these spectra were then divided by the running average of the average spectrum shown in the top left panel. The resulting flux ratios are plotted in the right-hand panels of Figure 13. In both panels, a component shifting from red to blue is evident. As was the case for the Hγ line, the modulations occur at high velocities (about 1750 km s^{-1}), which are about twice the velocity expected at the surface of a 0.6 $M_{\odot}$ white dwarf rotating at the spin period of 67.62 s. Both the continuum and line changes are consistent with the two-pole accretion scenario.

The location of UV emission lines in various types of cataclysmic variables has been studied with mixed results. Observations of eclipsing dwarf novae at high inclination (Szkody 1987; Mauche et al. 1994) have shown that the C iv line is generally not affected by the eclipse and hence originates from a large volume rather than close to the white dwarf. Studies of IPs such as EX Hya and FO Aqr (Mauche 1999; de Martino et al. 1999) have shown multiple emission regions. FO Aqr shows similarities to V455 And, with spin modulations in both the lines and continua but with amplitudes that vary with wavelength. De Martino et al. (1999) find both a hot component (∼37,000 K) associated with the inner regions of the accretion curtain or the heated polar regions of the white dwarf and a cooler 12,000 K component in the outer portions of the curtain that can extend out to 6 $R_{\rm wd}$. They also found changes in the spin modulation amplitudes over several years that they ascribed to changes in the size of the accretion curtain and azimuthal structure of the disk. Given that V455 And has a relatively high inclination so that the structure of the disk is important, and it is likely undergoing changes in the accretion curtains due to the outburst, it is difficult to pin down a particular model.

Using the data from October 10, the ratio of UV/optical amplitudes of the putative pulse period is about 3, similar to the ratio of 2.3 from the *GALEX* NUV and optical data (Silvestri et al. 2012). This ratio is also similar to that from COS and optical data on GW Lib at 3 yr past its outburst (Szkody et al. 2012). However, in GW Lib, the ratio increased to 5 at 4 yr past outburst, while in V455 And, it appears to decrease between 3 and 4 yr. The ratios after outburst all appear to be less than the typical ratios of 10–16 seen at quiescence (Szkody et al. 2002, 2007) in GW Lib and other accreting pulsating white dwarfs. Should the post-outburst variability in V455 And be due to non-radial pulsations, then the different UV/optical amplitude ratios could be understood as an indication of exciting different eigenmodes with different indices (see Robinson et al. 1995).

The UV/optical amplitude ratio for the spin period is 9 during both sets of observations of V455 And. This is a much larger value than the ratio of 2 found from the longer wavelength NUV

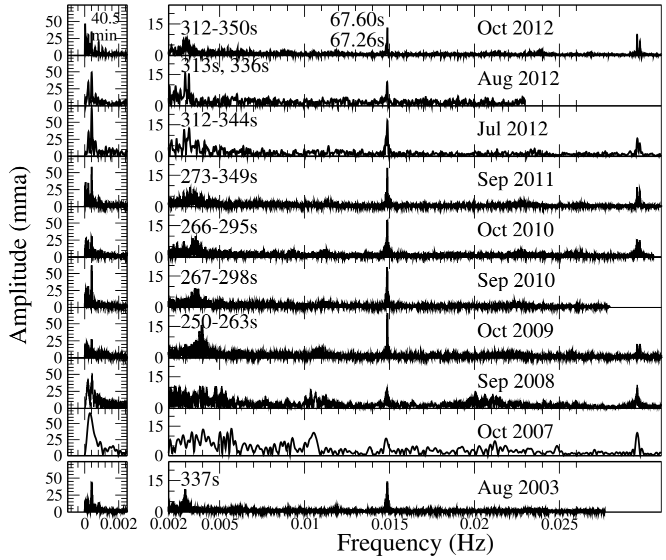

Figure 14. Combined DFTs from outburst (2007 October) to 5 yr past outburst (2012) showing the stability of the spin period but the progression of the ∼300 s period from shorter to longer periods as the time from outburst increases. The DFT at quiescence is shown at the bottom for comparison. Tables 1 and 2 provide the origin of the data.

data obtained in 2010 August and September. The difference is likely due to the greater S/N of the COS versus *GALEX* data; the COS data allow better time resolution to detect and resolve the spin periodicities. The large ratio of amplitudes argues for a location of the spin component close to, but hotter than, a 11,000 K white dwarf. This ratio must be used with some caution as the longer optical data sets allow for a resolution of the spin from the beat period, which can decrease its amplitude compared to the combined periods in the *HST* data. A ratio of 9 would be consistent with a white dwarf model of about 14,000 K (Szkody et al. 2010) and would also be consistent with the optical result of Bloemen et al. (2013), who concluded that the spin likely originates from the accretion curtains near the white dwarf, although they also could not produce any detailed model. This temperature is also in the range found by de Martino et al. (1999) for the accretion curtains of FO Aqr.

3.4. Long-term Trends

Figure 14 shows a compilation of DFTs using optical data obtained from one month (2007 October) to 5 yr (2012 October) past outburst as well as the DFT from quiescent data several years before the outburst (S. Pyrzas et al. in preparation). It is clear that the spin is weakly present even while the disk is still dominating the light at one month after the outburst, and then its amplitude increases dramatically by 2 yr past outburst when the disk is close to its quiescent level. The period of the spin is not noticeably altered by the outburst, but the amplitude ratio of the spin to its second harmonic reverses in the data soon after outburst.

In contrast, the broad range of periods ascribed to pulsations at quiescence disappears close to outburst and begins to re-appear by 2009 October, but at a shorter period range than apparent at quiescence. The observed periods drift to longer timescales as the time from outburst increases, approaching, but not yet identical to, the quiescent periods even at 5 yr post-outburst. This behavior is not unexpected if the origin is non-radial pulsations, as a change from short to long periods is consistent with excitation of different modes with rapid cooling of the outer envelope. Which pulsation modes are excited depends on the thermal timescale at the base of the convection zone (Brickhill 1992; Goldreich & Wu 1999; Wu 2001; Montgomery 2005), so as the star cools, the base moves deeper into the white dwarf. However, this slow drift in pulsation period at the rate of $d\nu/dt \sim -10^{-12}$ Hz s^{-1} (Townsley et al. 2004), from continued cooling of the outer envelope after outburst, is not evident in all the accreting white dwarfs that have been observed so far. EQ Lyn returned to exactly its pre-outburst pulsation spectrum within 3.3 yr following its outburst (Mukadam et al. 2011b). GW Lib showed two completely different periods in the 5 yr after its outburst (Szkody et al. 2012; Chote & Sullivan 2013) and still has not returned to its quiescent pulsation modes. V455 And has the coolest white dwarf among all the accreting pulsators and is one of the few that exist at a quiescent temperature that would place it in the instability strip for non-interacting DAV pulsators (Gianninas et al. 2005). Both EQ Lyn and GW Lib are much hotter at 15,000 K (Szkody et al. 2002; Mukadam et al. 2013). Arras et al. (2006) have suggested that these hotter systems could have increased He abundance and hence be unstable due to He II ionization. This difference in composition could lead to the different behaviors observed. Alternatively, the very fast rotation period of V455 And compared to the other accreting white dwarfs could influence its behavior. Townsley (2010) has shown that if the spin frequency is higher than the pulsation mode frequency, the Coriolis force alters the observed modes.

The major unsolved puzzle in ascribing this period to a non-radial pulsation of the white dwarf is why the spin period is so visible in the UV whereas the pulsation period is not, if they both originate from the white dwarf. The presence of the spin in the shortest wavelengths and in the emission lines argues for a location in the accretion curtains. If the ∼300 s period originates in these curtains or in the accretion disk itself, it is not clear how a period of this timescale could be sustained for years and how it would gradually shift from shorter to longer periods from 2 to 5 yr after outburst.

Ortega-Rodriguez & Wagoner (2007) explored non-radial *g*-mode disk oscillation modes in cataclysmic variables; however, their model was for optically thick, steady-state disks and the resulting oscillations are short (tens of seconds). Yamasaki et al. (1995) do produce periods in the range of 70–600 s with axially symmetric radial *p*-mode pulsations trapped in the outer part of an accretion disk, but this area could not explain the periodicity in the high-excitation UV emission lines of V455 And. There is a long history of observed periodicities in dwarf novae disks but none match the timescales of V455 And. Warner (2004) provides a review of these periods, which are termed dwarf nova oscillations (DNOs), longer period DNOs (termed lpDNOs), and quasi-periodic oscillations (QPOs). He argues that all of these are related to magnetic accretion. The DNOs could be caused by magnetic coupling to the equatorial accretion belt which is rotating at Keplerian velocities during a dwarf nova outburst. The lpDNOs appear to be related to the rotation of the white dwarf, where $P_{\mathrm{lpDNO}} \sim 1/2 P_{\mathrm{wd}}$ and $\sim 4 \times P_{\mathrm{DNO}}$. The QPOs can be explained by reprocessing or obscuration of the light from the hot inner regions by a slow moving prograde traveling wave in the inner disk that creates a vertical thickness of the disk. Theoretical support for such a wave was provided by Lubow & Pringle (1993), and Warner & Woudt (2002) postulate that this wave could be excited by the magnetic field interaction with the disk. The three-dimensional models of Romanova et al. (2003) of magnetic accretion onto an inclined rotating dipole have produced QPOs. While this magnetic model seems appropriate since V455 And shows the stable spin period (and its second harmonic) indicative of two pole accretion, the timescales do not appear to work out. In most dwarf novae, the DNOs are on the order of 10 s, the lpDNOs around 40 s, and the QPOs about 160 s. The Romanova et al. models produce QPOs that are $\leqslant P_{\rm wd}$. If there is no spun-up equatorial belt from the disk that would produce a short-period DNO in V455 And, and we use the spin period of 67.62 s in Equation (23) of Warner & Woudt (2002) where $P_{\rm QPO}/P_{\rm wd}$ = 10–19, we obtain QPO periods of 676–1284 s, much longer than those observed. If the timescales can be reproduced correctly, the magnetic model offers advantages, as the period changes could be related to the changing radius of the inner disk and the changing vertical height of a traveling wave could account for some obscuration that affects the QPO period but not the visibility of the accretion curtains where the spin period is observed.

4. CONCLUSIONS

Our UV and optical data on V455 And obtained following its 2007 dwarf nova outburst have provided insights as well as dilemmas. The results can be summarized as follows.

1. *HST* spectra at 3 and 4 yr past outburst show the white dwarf remained heated by several hundred degrees. Thus, the cooling time for large amplitude outbursts is greater than 4 yr. The optical spectra and photometry also showed increased fluxes over quiescent values at 3 yr past outburst but quiescent levels were reached by the fourth year. The cooling curve obtained from the white dwarf temperatures implies a mass $\sim 1.5 \times 10^{-9}\ M_{\odot}$ was accreted during the outburst.
2. The UV emission lines show large flux variability but no obvious correlation with the orbital period.
3. The spin period and its second harmonic show up within a month of outburst and are consistently present. The second harmonic has greater amplitude during the year following outburst. The strongest amplitudes of the spin and its second harmonic occur at wavelengths <1620 Å, and these periods are present in the UV emission lines as well. These results imply an origin from a hot component, possibly the accretion curtain close to the white dwarf. The UV continuum data folded on the spin period show a clear double-humped modulation consistent with two-pole accretion. The C IV emission line also shows changes in shape when phased on the spin period.
4. A range of periods that are similar to the 300–360 s observed at quiescence are apparent in the optical data following outburst, but gradually shift from 250–263 s when they appear 2 yr after outburst to 312–350 s by 5 yr after outburst. While a period in this range is evident in the UV continuum data at 3 yr past outburst, it is absent at 4 yr. Most surprisingly, this period is prominent in the UV emission lines in both years, indicating an origin away from the white dwarf photosphere.
5. While an association of the spin and 300 s periods with the accretion curtain appears plausible, it is not clear why the spin is clearly visible in the UV continuum whereas the putative pulsation is not. If this period originates in the hotter portions of the accretion curtain, the mechanism for producing a period in this range, sustainable for years and moving from long to short period as the white dwarf cools, is not clear.

The presence of permanent superhumps indicates the disk is eccentric, oscillating, and precessing. The strong presence of the spin period and its second harmonic points to an IP with a magnetic white dwarf and corresponding accretion curtains, as well as disk light, to take into account. While these components complicate the formulation of a good system model, the brightness of V455 And means that it can be easily observed from space and ground to provide the long-term data sets that can ultimately lead to a better understanding of the emission regions of a magnetic, rapidly rotating, possibly pulsating, accreting white dwarf.

We gratefully acknowledge Arlo Landolt and the observers of the AAVSO who contributed measurements during the course of the two sets of *HST* observations. This work was supported by NASA grants HST-GO1163.01A, HST-GO11639-01A, and HST-GO12231.01A from the Space Telescope Science Institute, which is operated by the Association of Universities for Research in Astronomy, Inc., for NASA, under contract NAS 5-26555, and by NSF grant AST-1008734. The research leading to these results has also received funding from the European Research Council under the European Union's Seventh Framework Programme (FP/2007–2013)/ERC Grant Agreement no. 267697 (WDTracer). B.T.G. was supported in part by the UK's Science and Technology Facilities Council (ST/1001719/1).

REFERENCES

Araujo-Betancor, S., Gänsicke, B. T., Hagen, H.-J., et al. 2005, A&A, 430, 629 (AB05)
Arras, P., Townsley, D. M., & Bildsten, L. 2006, ApJL, 643, L119
Bloemen, S., Steeghs, D., De Smedt, K., et al. 2013, MNRAS, 429, 3433
Brickhill, A. J. 1992, MNRAS, 259, 519
Broens, E., Vansteelant, D., Hautecler, H., et al. 2007, IAUC., 8876, 2
Chote, P., & Sullivan, D. J. 2013, in ASP Conf. Ser. 469, 18th European White Dwarf Workshop, ed. J. Krzesinski et al. (San Francisco, CA: ASP), 337
de Martino, D., Silvotti, R., Buckley, D. A. H., et al. 1999, A&A, 350, 517
Gänsicke, B. T. 2007, in ASP Conf. Ser. 372, 15th European Workshop on White Dwarfs, ed. R. Napiwotzki & M. R. Burleigh (San Francisco, CA: ASP), 597
Gänsicke, B. T., Dillon, M., Southworth, J., et al. 2009, MNRAS, 397, 2170
Gianninas, A., Bergeron, P., & Fontaine, G. 2005, ApJ, 631, 1100
Godon, P., Sion, E. M., Cheng, F., et al. 2006, ApJ, 642, 1018
Goldreich, P., & Wu, Y. 1999, ApJ, 511, 904
Hagen, H. J., Groote, D., Engels, D., & Reimers, D. 1995, A&AS, 111, 195
Howell, S. B., Szkody, P., & Cannizzo, J. 1995, ApJ, 439, 337
Hubeny, I. 1988, CoPhC, 52, 103
Hubeny, I., & Lanz, T. 1995, ApJ, 439, 875
Kepler, S. O. 1993, BaltA, 2, 515
Kepler, S. O., Costa, J. E. S., Castanheira, B. G., et al. 2005, ApJ, 634, 1311
Lubow, S. H., & Pringle, J. E. 1993, ApJ, 409, 360
Mauche, C. W. 1999, ApJ, 520, 822
Mauche, C. W., Raymond, J. C., Buckley, D. A. H., et al. 1994, ApJ, 424, 347
Montgomery, M. H. 2005, ApJ, 633, 1142
Mukadam, A. S., Owen, R., Mannery, E., et al. 2011a, PASP, 123, 1423
Mukadam, A. S., Townsley, D. M., Szkody, P., et al. 2011b, ApJL, 728, L33
Mukadam, A. S., Townsley, D. M., Szkody, P., et al. 2013, AJ, 146, 54
Nather, R. E., & Mukadam, A. S. 2004, ApJ, 605, 846
Ortega-Rodriguez, M., & Wagoner, R. V. 2007, ApJ, 669, 1158
Piro, A., Arras, P., & Bildsten, L. 2005, ApJ, 628, 401
Robinson, E. L., Mailloux, T. M., Zhang, E., et al. 1995, ApJ, 438, 908
Romanova, M. M., Ustyugova, G. V., Koldoba, A. V., Wick, J. V., & Lovelace, R. V. E. 2003, ApJ, 595, 1009
Samus, N. N., Broens, E., Diepvens, A., Hautecler, H., & Vansteelant, D. 2007, IAUC, 8868, 2
Silvestri, N. M., Szkody, P., Mukadam, A. S., et al. 2012, AJ, 144, 84
Sion, E. M., Szkody, P., Mukadam, A., et al. 2013, ApJ, 772, 116
Szkody, P. 1987, AJ, 94, 1055
Szkody, P., Gänsicke, B. T., Howell, S. B., & Sion, E. M. 2002, ApJL, 575, L79
Szkody, P., Mukadam, A., Gänsicke, B. T., et al. 2007, ApJ, 658, 1188

Szkody, P., Mukadam, A., Gänsicke, B. T., et al. 2010, ApJ, 710, 64
Szkody, P., Mukadam, A. S., Gänsicke, B. T., et al. 2012, ApJ, 753, 158
Townsley, D. M. 2010, Physics of Accreting Compact Binaries, UAP, in press
Townsley, D. M., Arras, P., & Bildsten, L. 2004, ApJL, 608, L105
Townsley, D. M., & Bildsten, L. 2003, ApJL, 596, L227
Townsley, D. M., & Gänsicke, B. T. 2009, ApJ, 693, 1007
Warner, B. 2004, PASP, 116, 115
Warner, B., & Woudt, P. 2002, MNRAS, 335, 84
Wu, Y. 2001, MNRAS, 323, 248
Yamasaki, T., Kato, S., & Mineshige, S. 1995, PASJ, 47, 59